Preclinical Development

Molecular Cancer Therapeutics

Synthetic Lethal Screening with Small-Molecule Inhibitors Provides a Pathway to Rational Combination Therapies for Melanoma

Devin G. Roller[1], Mark Axelrod[1], Brian J. Capaldo[2], Karin Jensen[3], Aaron Mackey[2,4], Michael J. Weber[1,4], and Daniel Gioeli[1,4]

Abstract

Recent data show that extracellular signals are transmitted through a network of proteins rather than hierarchical signaling pathways, suggesting that the inhibition of a single component of a canonical pathway is insufficient for the treatment of cancer. The biologic outcome of signaling through a network is inherently more robust and resistant to inhibition of a single network component. In this study, we conducted a functional chemical genetic screen to identify novel interactions between signaling inhibitors that would not be predicted on the basis of our current understanding of signaling networks. We screened over 300 drug combinations in nine melanoma cell lines and have identified pairs of compounds that show synergistic cytotoxicity. The synergistic cytotoxicities identified did not correlate with the known *RAS* and *BRAF* mutational status of the melanoma cell lines. Among the most robust results was synergy between sorafenib, a multikinase inhibitor with activity against RAF, and diclofenac, a nonsteroidal anti-inflammatory drug (NSAID). Drug substitution experiments using the NSAIDs celecoxib and ibuprofen or the MAP–ERK kinase inhibitor PD325901 and the RAF inhibitor RAF265 suggest that inhibition of COX and mitogen-activated protein kinase signaling are targets for the synergistic cytotoxicity of sorafenib and diclofenac. Cotreatment with sorafenib and diclofenac interrupts a positive feedback signaling loop involving extracellular signal–regulated kinase, cellular phospholipase A2, and COX. Genome-wide expression profiling shows synergy-specific downregulation of survival-related genes. This study has uncovered novel functional drug combinations and suggests that the underlying signaling networks that control responses to targeted agents can vary substantially, depending on unexplored components of the cell genotype. *Mol Cancer Ther; 11(11); 2505–15. ©2012 AACR.*

Introduction

The promise of targeted therapy is that the identification of genetic changes that underlie malignancy, and the rational development of drugs that interdict those changes, will yield effective treatments with minimal toxicity (1). This approach has been spectacularly successful in the treatment of chronic myelogenous leukemia (CML) with inhibitors of Bcr-Abl (2), but this success has not been widely replicated (3). Many oncogenic "drivers" are difficult to target directly (e.g., *P53* and *RAS*). Moreover, even in cases where a primary driver is targeted effectively, such as inhibition of mutated *EGFR* or *BRAF*, responses to single-agent therapies are usually partial or do not endure (4, 5). In these cases, resistance emerges due to the selection of cells that express mutant forms of the target protein that no longer are sensitive to the drug or by the expression of signaling activities that compensate for the inhibition of the primary target (6, 7).

There is increasing interest in identifying combinations of therapies that will enhance the efficacy of targeted therapies. Thus, numerous attempts have been made to combine a targeted drug with a cytotoxic drug or with a molecule that would enhance the likelihood of apoptosis (8). However, it has become clear that the targeted therapy itself can induce the expression of compensatory progrowth and prosurvival activities. This implies that inhibition of one or more of these compensatory pathways could enhance the efficacy of the primary targeted therapy. There are early indications to support this. For example, in our own work, we observed that treatment of prostate cancer xenografts with the MAP–ERK kinase (MEK) inhibitor, PD325901, induced the expression of genes in the mitogen-activated protein kinase (MAPK), phosphoinositide 3-kinase (PI3K), and Hedgehog pathways, and also enhanced activation of members of those pathways as well as NF-κB (9). Cotreatment of prostate

Authors' Affiliations: Departments of [1]Microbiology, Immunology, and Cancer Biology, [2]Public Health Sciences, [3]Biomedical Engineering, and [4]Cancer Center, University of Virginia, Charlottesville, Virginia

Note: Supplementary data for this article are available at Molecular Cancer Therapeutics Online (http://mct.aacrjournals.org/).

Corresponding Author: Daniel Gioeli, Department of Microbiology, Immunology, and Cancer Biology, University of Virginia, Jordan Hall Rm 2-16, Box 800734, 1300 Jefferson Park Avenue, Charlottesville, VA 22908. Phone: 434-982-4243; Fax: 434-982-0689; E-mail: dgioeli@virginia.edu

doi: 10.1158/1535-7163.MCT-12-0461

cancer cell lines with the MEK inhibitor and any one of the alternative compensatory pathways led to synergistically enhanced cytotoxicity.

Combinations of targeted therapies have potential use both in cases where one of the drugs directly inhibits a mutated driver and where the mutated driver cannot be directly targeted. For example, *RAS*-driven tumors could, in theory, be treated with RAF inhibitors, which block the downstream pathway. However, resistance mechanisms analogous to those that arise in *RAF*-driven tumors are likely also to appear in *RAS*-driven cancers. Thus, understanding the ways signaling pathways interact to form a robust network could aid construction of rational drug combinations in a broad variety of contexts.

To systematically identify pathways that would be appropriate for cotargeting, we assembled a library of signal transduction inhibitors focused on small molecules that were either U.S. Food and Drug Administration (FDA)-approved anticancer drugs, potential drugs in early phase development, or tool compounds that inhibit pathways and molecules of known targets for anticancer drug development. We have screened this library, in single and pairwise combinations, against a panel of melanoma cell lines that represent its major known genotypes (Supplementary Table S1). We searched for combinations that would cause synergistic cytotoxicity (based on Bliss independence; refs. 10, 11) to focus on those pathways that were functionally linked. We found that only a limited set of combinations were synergistic, and none of the combinations were synergistic in all cell lines, supporting the hypothesis that this methodology selects for specific pathways rather than general cytotoxic responses. Among the most robust and surprising of these synergistic combinations was the multikinase inhibitor sorafenib combined with the anti-inflammatory drug diclofenac. This combination was synergistic in melanomas with mutations in *BRAF*, *NRAS*, or neither mutation, suggesting the existence of a subset of melanomas that share commonalities in the organization of their signaling networks, regardless of primary driver mutation. Drug substitution studies indicated that the MAPK pathway and the COX pathway were important components of this synergy. Genome-wide expression studies further showed both common and distinct aspects of synergy-specific downregulation of survival-related genes. Thus, this approach has identified COX as a potential survival mechanism for cells undergoing receptor tyrosine kinase (RTK)–MAPK blockade. Moreover, it provides proof-of-principle that synthetic lethal screening with small molecules can be used to identify novel functional drug combinations.

Materials and Methods

Cell cultures, antibodies, and reagents

MeWo, SkMel2, SkMel28 cells (American Type Culture Collection), A375, VMM5A, VMM39, SLM2, DM122, DM331 (kind gift from Dr. Craig Slingluff, University of Virginia, Charlottesville, VA; ref. 12), and SLM2 (kind gift from Dr. Angela Zarling, University of Virginia) were propagated in RPMI-1640 (Invitrogen) supplemented with 5% or 10% FBS (Gemini Bio-Products). All cultures were maintained in a humidified chamber at 37°C with 5% CO_2. An OncoMap analysis was conducted at the Broad Institute (Cambridge, MA) to identify the mutational status of over 30 known oncogenes and tumor suppressor genes (13). The cell lines were authenticated by comparing the tumor mutation profile determined by OncoMap with published reports.

Antibodies were obtained from the following sources: anti-phosphoERK (Sigma-Aldrich), antitubulin (Calbiochem), anti-ERK (B3B9) from the UVa hybridoma facility, anti–cellular phospholipase A2 (cPLA2; Cell Signaling Technology), and anti–phospho-cPLA2 (Santa Cruz Biotechnology).

The following small-molecule inhibitors were obtained from EMD Chemicals: 5-aza-2-deoxycytidine, AACOCF$_3$, AG490, AKT inhibitor IX, AMPK inhibitor, anacardic acid, celecoxib, cyclopamine-KAAD, D4476, diclofenac Na, DMAT, DNA-dependent protein kinase inhibitor, geldanamycin, GM6001, H-89, indirubin-3′-monoxime, IP3 kinase inhibitor, Jak I inhibitor, K-252c, ML-7, NDGA, okadaic acid, olomoucine, PD173074, S3I-201, SANT-1, SB203580, SC-514, sphingosine kinase inhibitor, STO-609, SU6656, TGF-α receptor II inhibitor, trichostatin A, TX-1918, U0126, withaferin A, wortmannin, and WP1066. Bortezomib, dasitinib, erlotinib, gefitinib, imatinib, lapatinib, lestaurtinib, nilotinib, rapamycin, sorafenib, sunitinib, temsirolimus, and vandetanib were acquired from LC Laboratories (Woburn, MA). 5-AIQ-hydrochloride, bevacizumab, D609 Prodrug, GF109203X, GW441756, picropodophyllotoxin (PPP), and SP600125 were obtained from Sigma-Aldrich. Debromohymeniadlisine was purchased from Enzo Life Sciences. OSU-03012 was obtained from Cayman Chemical. Y27632 dihydrochloride was acquired from Tocris Bioscience. PD325901 was a gift from Pfizer. Slo-101 was a gift from Dr. Deborah Lannigan (University of Virginia). Compounds were diluted in vehicle as specified by the manufacturer. IFN-α was a gift from Dr. Craig Slingluff (University of Virginia), and suberoylanilide hydroxamic acid was a gift from Dr. David Jones (University of Virginia).

Synthetic lethal pathway screen

Cell lines were grown in their normal growth media to 80% confluence and then washed with 1× PBS, trypsinized, collected, counted (via hemacytometer), and resuspended in phenol red–free RPMI-1640 + 5% FBS at concentrations that would result in 100% confluence of the vehicle-treated control wells after 3 days of growth. Plating of the cells was carried out using the BioMek NX (Beckman Coulter) workstation. Ninety microliters of cell suspension was added per well in 96-well format. Small-molecule inhibitors were diluted to 10 times the concentration and plated by hand into master drug plates. The BioMek NX workstation was used to add 10 μL of drug from the master plates to each well. The cells were then incubated for 3 days at 37°C

and 5% CO_2. Following this incubation, the BioMek NX workstation was used to add 10 μL of alamarBlue (Invitrogen) to each well. The plates were incubated for 4 hours and fluorescence was measured at 560 nm excitation/590 nm emission on a Synergy 2 plate reader (BioTek Instruments). Mean results and SE were calculated for triplicate samples.

Cytotoxicity assays

alamarBlue. Four hours after being plated in 96-well plates, cells were treated with inhibitors or vehicle control in phenol red–free RPMI-1640 (Invitrogen) without FBS and incubated for 3 days at 37°C. alamarBlue (Invitrogen) was added to wells and incubated for 4 hours at 37°C. Fluorescence was measured as described earlier.

Crystal violet. Cells were allowed to adhere to 12-well plates overnight before being treated with inhibitors or vehicle control in phenol red–free RPMI-1640 (Invitrogen) without FBS for 7 days at 37°C. Plates were placed on ice and media was aspirated off cells. Cells were rinsed twice with cold 1× PBS (Invitrogen) and fixed with cold 100% methanol for 10 minutes. Monolayers were stained with 0.5% crystal violet in 25% methanol:water for 10 minutes at room temperature and rinsed with distilled water until excess crystal violet solution had been removed. Plates were inverted to allow cells to air-dry overnight. Micrographs were taken with a Nikon SMZ1000 microscope equipped with a Nikon Coolpix 4300 digital camera. Digital images were processed with Adobe Photoshop CS2 version 9.0.2.

Immunoblot and immunoprecipitation analysis

Cells were allowed to adhere to plates overnight before being treated with inhibitors or vehicle control in phenol red–free RPMI-1640 (Invitrogen) without FBS for 1 hour at 37°C. Cells were rinsed with cold 1× PBS and lysed in Triton lysis buffer [10% Triton X-100, 5% 1 mol/L Tris (pH 7.5), 2.5% 4 mol/L NaCl, 0.5% 0.5 mol/L NaF, 0.01% 0.5 mol/L EDTA, 80% water] plus the following protease and phosphatase inhibitors: 1 μg/mL pepstatin, 1 μg/mL leupeptin, 0.4 trypsin inhibitor unit/mL aprotinin, 1 mmol/L phenylmethylsulfonyl fluoride, 200 μmol/L orthovanadate, 50 mmol/L β-glycerophosphate, and 0.4 μmol/L microcystin. Lysates were centrifuged at 13,000 rpm at 4°C for 10 minutes and supernatants were collected. Protein concentrations were determined using BCA protein assay (Thermo Scientific). Protein extracts were prepared with Triton lysis buffer and Laemmli Sample Buffer/β-mercaptoethanol, boiled, loaded into acrylamide gels, and then run at 75 V for 30 minutes then at 125 V for 1 hour. Gels were transferred onto nitrocellulose membranes at 90 V for 60 minutes at 4°C. Membranes were stained with Ponceau red and then were blocked with 5% bovine serum albumin in PBS-T for 1 hour. Blots were incubated overnight at 4°C in primary antibodies, washed with PBS-T, incubated in a secondary antibody (LI-COR) for 1 hour at room temperature, and imaged using the Odyssey Infrared Imaging System (LI-COR). Quantification was done using the Odyssey software and mean results and SE were calculated for triplicate samples.

For immunoprecipitation analysis, protein extracts were incubated with antibody at 4°C overnight. Agarose beads (Roche) were washed with Triton lysis buffer with protease inhibitors and were added to the sample antibody solution and incubated for 4 hours at 4°C. The beads were then washed with Triton lysis buffer with protease and phosphatase inhibitors, resuspended in Laemmli Sample Buffer/β-mercaptoethanol, and loaded into acrylamide gels. Gels were run, transferred, and immunoblotted as described earlier with the following exception: membranes were washed with TBS-T.

Gene array

SLM2, VMM39, and DM331 cells were plated and incubated overnight before being treated, in duplicate, with inhibitors or vehicle control in phenol red–free RPMI-1640 without FBS for 8 hours at 37°C. Cells were placed on ice and rinsed with cold 1× PBS. Cells were collected and RNA was isolated using the Qiashredder (Qiagen) and RNeasy Mini Kit (Qiagen). The gene array was conducted using Illumina 3′IVT human HT-12 BeadChip arrays by Gene Analysis. Principal component analysis and clustering quality control analyses of the results indicated that 2 of the inhibitor-treated DM331 samples exhibited irregular quantities unseen in the majority of samples, leading us to conservatively exclude all DM331 sample results from further analyses. Differential expression analyses of quantile-normalized, $\log_2$-transformed expression values were conducted using moderated ANOVA hypothesis testing (14), as provided by the R/BioConductor (15) limma package (16), with Benjamini–Hochberg corrections for multiple hypothesis testing to control false discovery rate (FDR). All microarray data have been deposited with the National Center for Biotechnology Information Gene Expression Omnibus under accession GSE39192.

Results

Screening for synergistic signaling interactions

We assembled a library of 60 small-molecule inhibitors that target proteins in diverse signaling pathways. In selecting these inhibitors, we focused on chemicals that were either FDA-approved, in clinical trial, or that targeted pathways for which there are FDA-approved drugs. The library included inhibitors of RTKs [EGF receptor (EGFR), insulin-like growth factor receptor (IGFR), VEGF receptors (VEGFR)], and intracellular kinases [MEK, SRC, protein kinase C, PI3K, cyclin-dependent kinases (CDK), mTOR, protein kinase A]. We also used inhibitors of other cellular enzyme classes [histone deacetylases (HDAC), lipoxygenases, COXs, and topoisomerases] as well as chemotherapy agents. Using this library, we probed cell signaling networks to discover functional relationships within this diverse set of compounds.

In a 96-well monolayer format using the Biomek NX high-throughput workstation, we conducted a series of optimization experiments to determine the appropriate cell number and growth conditions (data not shown) for each of 9 melanoma cell lines that differ in genetic profile and are representative of the major known genetic alterations in melanoma (*BRAF*, *NRAS*, and wild-type). The cell plating and drug addition were conducted robotically using the Biomek and growth inhibition was measured with alamarBlue. Five drugs with primary activity against EGFR, IGFR, RAF, MEK, and mTOR were designated as primary drugs and screened against 60 compounds in our library of small-molecule inhibitors. The results of the screen, summarized by synergy or antagonism compared with a Bliss prediction of independence is shown in Fig. 1A. The columns denote different drug combinations, the rows the different melanoma cell lines, and the color the degree of synergy or antagonism according to a model of Bliss independence (10, 11). The Bliss model of independence estimates the combined effect of 2 drugs as the multiplicative effect of each drug measured individually (1 − effect drug 1 × effect drug 2). We scored the top 5% of drug combinations with the greatest synergy as hits (Fig. 1B). This 5% cutoff selected drug combinations with growth inhibition of 24% or greater than that predicted by Bliss independence. This is described in detail for one drug combination later and in Fig. 2.

A cluster analysis of all of the hits from the screen (Fig. 1C) shows that many drug combinations were synergistic in a single cell line although many combinations were synergistic across multiple cell lines. The cells showing synergy did not cluster according to *RAS* or *RAF* mutational status, which was determined by OncoMap (13). For example, 2 V600E mutant lines, VMM12 and VMM18

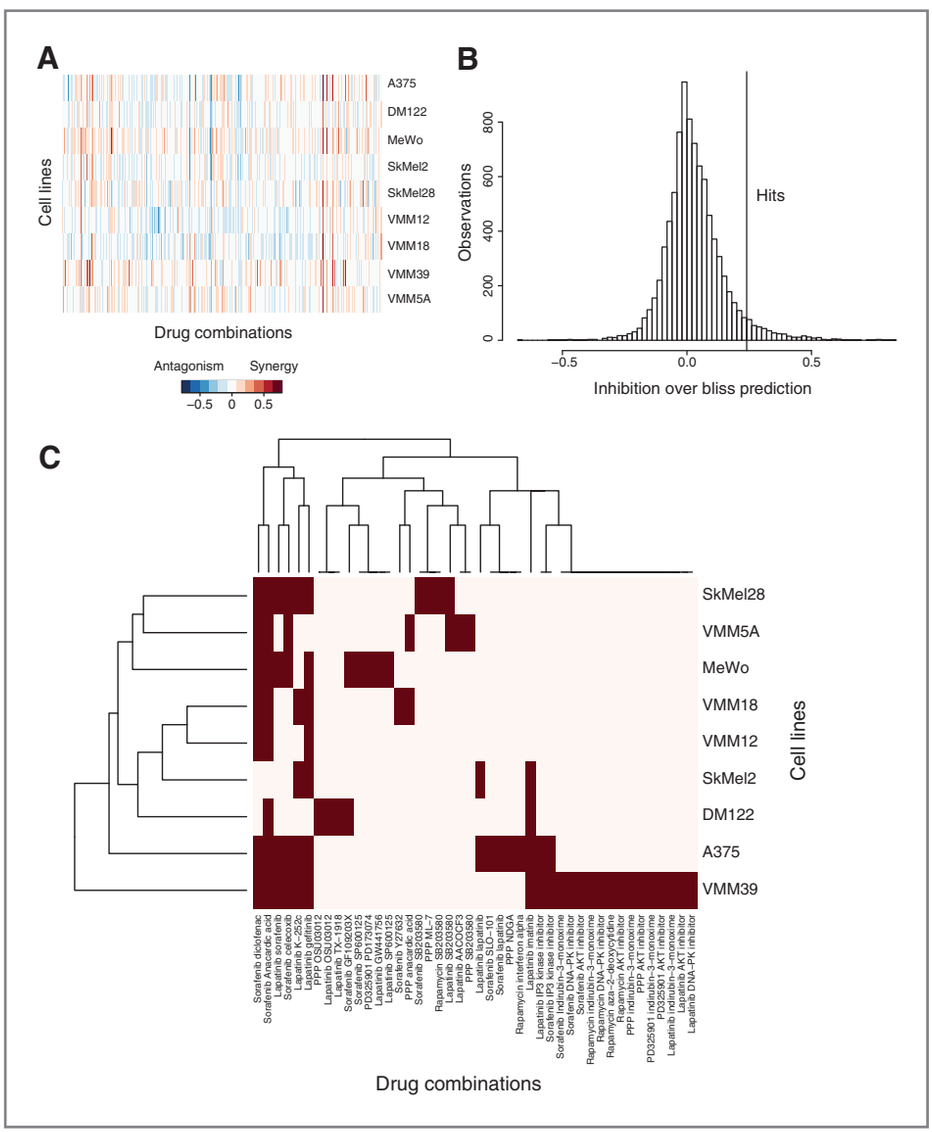

Figure 1. Synthetic lethality screen identifies synergistic and antagonistic drug pairs in melanoma cell lines. A, screen results shown as inhibition beyond Bliss independence prediction. Positive values indicate synergy and negative values indicate antagonism. Columns denote drug combinations, rows denote cell lines, and color denotes the difference between measured inhibition and Bliss prediction. B, distribution of Bliss differences for all drug combinations in screen ($n = 8{,}862$). Hits are defined as the top 5% of combinations with the highest additivity over Bliss independence prediction. C, clustergram of drug combinations defined as hits (red). Cell lines and drug combinations are clustered by complete linkage.

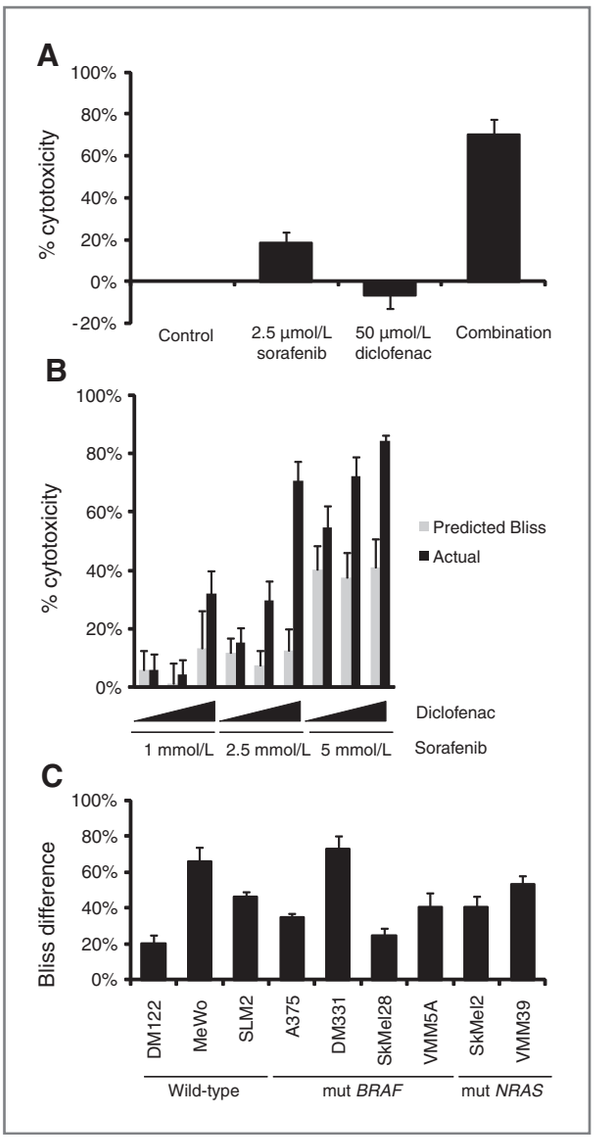

Figure 2. Sorafenib and diclofenac cause synergistic cytotoxicity. A, B-raf mutant cells DM331 were treated with vehicle control, 2.5 μmol/L sorafenib, 50 μmol/L diclofenac, or concurrent treatment of 2.5 μmol/L sorafenib, and 50 μmol/L diclofenac for 3 days. Metabolic activity was read out using alamarBlue ($n = 9$). B, DM331 cells were concurrently treated with sorafenib (1 μmol/L, 2.5 μmol/L, or 5 μmol/L) and diclofenac (10 μmol/L, 25 μmol/L, or 50 μmol/L) for 3 days. alamarBlue was used to read out metabolic activity. Predicted Bliss (gray bars) and actual additivity are displayed for each dose combination ($n = 10$). C, wild-type for both *NRAS* and *BRAF* cells: DM122, MeWo, and SLM2; *BRAF* mutant cells: A375, DM331, SKMel28, and VMM5A; and *NRAS* mutant cells: SKMel2 and VMM39 were treated with combinations of sorafenib and diclofenac for 3 days. alamarBlue was used to read out metabolic activity, and the Bliss difference was calculated by subtracting the calculated Bliss from the actual additivity ($n \geq 3$).

clustered together, however, the next closest cell lines were the *NRAS* mutant SkMel2 and the double wild-type DM122 where double wild-type denotes wild-type for both *RAF* and *RAS*. Furthermore, no drug combination generated synthetic lethality selectively in the *RAF* or *RAS* mutant cell lines. These results suggest the importance of the global genetic background in determining drug synergy.

One intriguing and surprising example that shows synergy is the combination of sorafenib, a multikinase inhibitor with RAF activity, and the anti-inflammatory COX inhibitor diclofenac. We also observed similar, although less robust, results in our screen with celecoxib in combination with sorafenib, suggesting that diclofenac was acting as a COX inhibitor. The sorafenib and diclofenac combination showed synergy in most cell lines tested at physiologically relevant doses (17, 18). Both drugs are well tolerated and FDA approved (19, 20). Synergy with sorafenib and diclofenac did not correlate with *RAS* or *RAF* mutational status of the cell lines. We selected this drug combination for further analysis because of its robustness and wide use.

In subsequent experiments, we confirmed Bliss synergy and the level of cytotoxicity for sorafenib and diclofenac. The greater effect of the drug combination over the individual drugs is illustrated in Fig. 2A. In the V600E *RAF* mutant cell line, DM331, 2.5 μmol/L sorafenib generated less than 20% cytotoxicity and 50 μmol/L diclofenac had no effect on growth. However, the combination treatment with those same doses generated over 75% cytotoxicity in DM331 cells. For 2.5 μmol/L sorafenib and 50 μmol/L diclofenac in DM331 cells, the predicted Bliss model of independence is 20% ($1 - 0.80 \times 1$). The actual observed effect of this drug combination's dose was 75%, indicative of synergy. Synergy was observed for multiple sorafenib and diclofenac doses (Fig. 2B). We define the Bliss difference as the numerical difference between the actual observed percentage cytotoxicity and the percentage cytotoxicity predicted by the Bliss model of independence. We observed synergy with sorafenib and diclofenac in all melanoma cell lines tested although the magnitude varied (Fig. 2C).

Because alamarBlue is a measure of cell metabolism, we wanted to use a more direct measure to confirm that sorafenib and diclofenac induced synergistic cell death. Melanoma cells were treated with sorafenib and diclofenac, singly or in combination, and stained 3 days later with crystal violet as a surrogate for cell number (Supplementary Fig. S1). Diclofenac alone had minimal to no effect on the cells and sorafenib decreased the number of cells. Combinatorial treatment with sorafenib and diclofenac led to a dramatic loss of cells.

Mechanisms of synergy for sorafenib and diclofenac

While most of the inhibitors used in our synthetic lethal screen are marketed as specific for a single cellular target, it is likely that many of the compounds have off-target effects where the drug inhibits more than 1 cellular target (21–23). Sorafenib is known to inhibit multiple kinases and diclofenac may inhibit more than just COX1 and COX2. To determine whether synergistic growth inhibition was due to off-target effects, we substituted drugs of

different chemical structure but similar pathway specificity. Both celecoxib and ibuprofen qualitatively substituted for diclofenac in combination with sorafenib, showing a Bliss difference across multiple melanoma cell lines with different genetic backgrounds for *BRAF* and *NRAS* mutational status (Fig. 3A and B). The magnitude of Bliss difference was greatest with diclofenac, followed by celecoxib and then ibuprofen (compare Figs. 2C, 3A and B). This quantitative difference may be due to the relative selectivity of these drugs for COX1 and COX2, in which ibuprofen is the least selective for COX2. These experiments suggest that the synergy displayed by sorafenib and diclofenac is due, at least in part, to diclofenac inhibition of COX activity.

We conducted similar drug substitution experiments for sorafenib, substituting the highly selective MEK inhibitor, PD325901, or the more selective RAF inhibitor derived from sorafenib, RAF265, in combination with diclofenac (Fig. 3C and D). Qualitatively, these drugs substituted for sorafenib although, again, the Bliss difference was quantitatively less than that achieved with sorafenib plus diclofenac. PD325901 plus diclofenac yielded greater Bliss differences across more melanoma cell lines than RAF265 plus diclofenac. These data suggest that sorafenib inhibition of the MAPK pathway contributes to the synergy observed with the sorafenib plus diclofenac combination. However, other sorafenib targets likely contribute to the observed synergy as well.

To determine whether the synergy was caused by increased inhibition of the MAPK pathway, or by enhanced sensitivity of cells to MAPK inhibition, we measured the effect of diclofenac on the ability of sorafenib to inhibit levels of phospho-ERK. Short-term treatment of melanoma cells with sorafenib or PD325901 decreased extracellular signal–regulated kinase (ERK) phosphorylation in a dose-dependent manner in all cell lines examined. Surprisingly, the ID_{50} for phospho-ERK was reduced by diclofenac in the BRAF mutant cell lines, but not in the mutant *RAS* or wild-type cell lines (Fig. 4 and data not shown). Thus, the mechanism of synergy differed in BRAF mutant melanoma lines from the other lines tested.

In DM331 cells harboring a mutant BRAF, 2.5 μmol/L sorafenib alone decreased pERK by 56%, whereas 50 μmol/L diclofenac alone did not inhibit pERK activity (Fig. 4A and B). The combination of sorafenib and

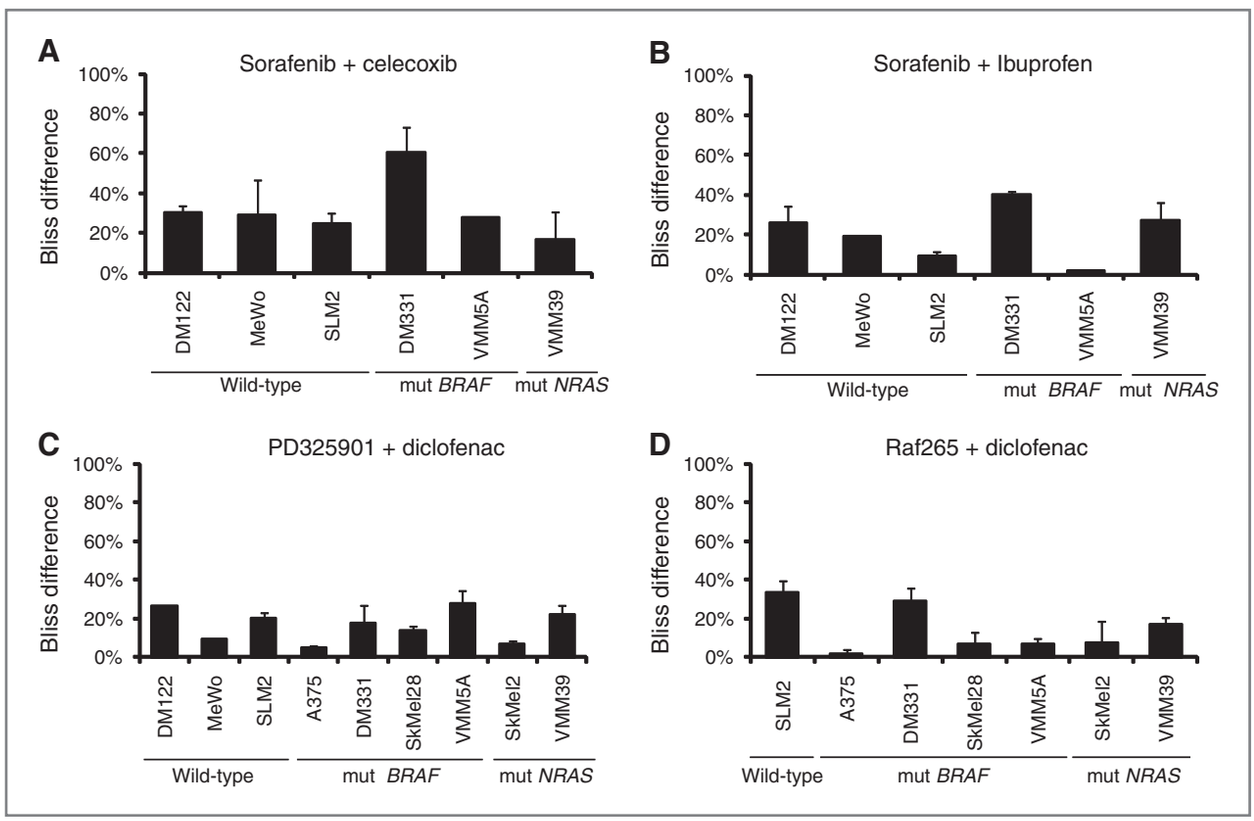

Figure 3. Inhibition of COX and MEK signaling are involved in the synergistic cytotoxicity observed with sorafenib and diclofenac. *NRAS* and *BRAF* wild-type cells: DM122, MeWo, and SLM2; *BRAF* mutant cells: DM331 and VMM5A; and *NRAS* mutant cells: VMM39 were concurrently treated with sorafenib and celecoxib (A) or sorafenib and ibuprofen (B). C, *NRAS* and *BRAF* cells wild-type cells: DM122, MeWo, and SLM2; *BRAF* mutant cells: A375, DM331, SkMel28, and VMM5A; and *NRAS* mutant cells: SkMel2 and VMM39 were concurrently treated with PD325901 and diclofenac. D, *NRAS* and *BRAF* cells wild-type cells: SLM2; *BRAF* mutant cells: A375, DM331, SkMel28, and VMM5A; and *NRAS* mutant cells: SkMel2 and VMM39 were concurrently treated with RAF265 and diclofenac. Cells were treated for 3 days. alamarBlue was used to read out metabolic activity and the Bliss difference was calculated as in Fig. 2 ($n \geq 3$).

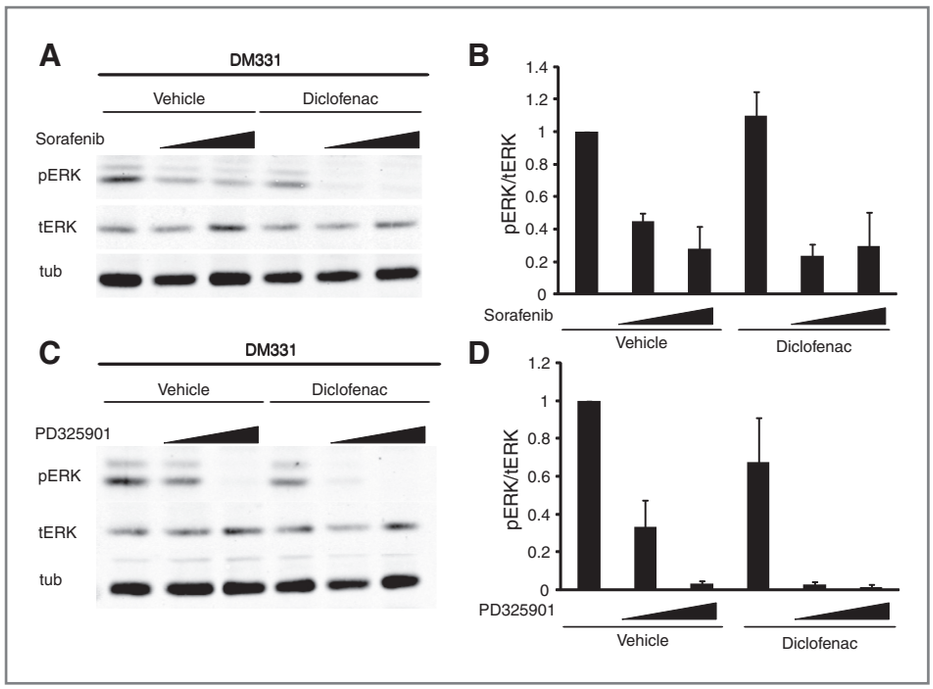

Figure 4. The effect of drug combinations on ERK activity. Total protein was isolated and immunoblot analyses for pERK, tERK, and tubulin were conducted from cells treated as follows: A, DM331 were incubated with vehicle, 2.5 μmol/L sorafenib, 5 μmol/L sorafenib, 50 μmol/L diclofenac, or sorafenib and diclofenac for 1 hour. B, quantification of Western blot analysis ($n \geq 4$). C, DM331 cells incubated with vehicle, 1 nmol/L PD325901, 5 nmol/L PD325901, 50 μmol/L diclofenac, or PD325901 and diclofenac for 1 hour. D, quantification of Western blot analysis ($n = 3$).

diclofenac at these doses decreased pERK signaling by 76%. Bliss independence predicts 50% inhibition of pERK at 2.5 μmol/L sorafenib and 50 μmol/L diclofenac. Thus, the observed inhibition of pERK exceeds what is predicted by Bliss independence indicating synergistic inhibition (Fig. 4B, compare 2nd and 5th bars). Increasing the dose of sorafenib to 5 μmol/L results in additive inhibition of pERK when combined with diclofenac (Fig. 4B). A parallel effect occurred when using PD325901 in place of sorafenib (Fig. 4C and D); 1 nmol/L PD325901 inhibited pERK by 67% and when combined with 50 μmol/L diclofenac pERK was inhibited by 97% (Fig. 3D, compare 2nd and 5th bars). This observed inhibition of pERK exceeded that predicted by Bliss independence denoting synergy. Using a higher dose of PD325901 (2.5 nmol/L) resulted in additive inhibition of pERK when combined with diclofenac. Collectively these data suggest that in the *BRAF* mutant DM331 cell line, pERK activity is synergistically inhibited by the combination of sorafenib and diclofenac in a dose-dependent manner.

A positive feedback relationship exists between ERK and COX signaling. It is known that prostaglandin E_2 (PGE_2) is able to activate the RAS–MAPK pathway (24, 25). Conversely, ERK can activate cPLA2 by phosphorylation at S505, enhancing the hydrolysis of membrane phospholipids to release arachidonic acid (26). COX then metabolizes arachidonic acid into eicosanoids, such as PGE2 (27). We therefore determined whether sorafenib and diclofenac altered cPLA2 phosphorylation on S505 (Fig. 5). The addition of 2.5 μmol/L sorafenib or 50 μmol/L diclofenac each slightly reduced phospho-cPLA2 levels, 27% and 36%, respectively. The combination of sorafenib and diclofenac further reduced phospho-cPLA2 levels, inhibiting phospho-cPLA2 by 65%. This exceeds the level of inhibition predicted by Bliss independence (52%) and indicates synergistic inhibition of phospho-cPLA2 and is consistent with ERK and COX feed forward signaling.

Because ERK was not synergistically inhibited by sorafenib and diclofenac in the VMM39 or SLM2 cell lines, we turned to gene expression analysis to elucidate the underlying mechanism(s) leading to synergistic cytotoxicity in these cell lines. Both VMM39 and SLM2 displayed significantly different basal gene transcription profiles consistent with the different mutational status of *RAS* and *BRAF* in the cell lines; VMM39 cells are *NRAS* mutant and SLM2 cells are double wild-type. Treatment of either cell line with the individual drugs had little effect on gene expression, consistent with the low cytotoxicity of single drug administration. At a 1% FDR, there were no transcriptional changes in response to 50 μmol/L diclofenac in either SLM2 or VMM39; there were also no transcriptional changes in SLM2 in response to 5 μmol/L sorafenib at 24 hours. At a 1% FDR, the transcription of only 18 genes was altered in VMM39 cells in response to sorafenib. A heatmap of the significant genome-wide changes in VMM39 and SLM2 transcription in response to single drug and combination treatment is shown in Fig. 6. The combination of sorafenib and diclofenac generated significant transcriptional changes; for each cell line [compare the last 2 columns in the heatmap (Fig. 6) to the preceding 6 columns]. Four different patterns of transcriptional responses emerge from the combination of sorafenib and diclofenac. Some genes are downregulated by the combination in both VMM39 and SLM2 (Fig. 6, group B)

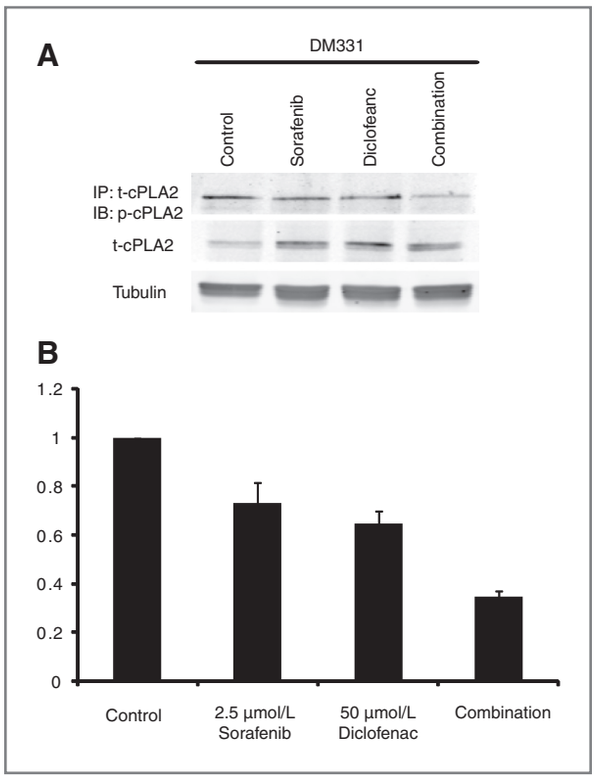

Figure 5. The effect of drug combinations on cPLA2 activity. Total protein was isolated and immunoprecipitation analysis was conducted for tcPLA2. These samples were blotted for phosph-CPLA2. Immunoblot analyses for total-cPLA2 and tubulin were also conducted from cells treated as follows: A, DM331 were incubated with vehicle, 2.5 μmol/L sorafenib, 5 μmol/L sorafenib, 50 μmol/L diclofenac, or sorafenib and diclofenac for 1 hour. B, quantification of Western blot analysis ($n = 3$).

although with varying magnitude. There are also many genes that are upregulated by the combination of sorafenib and diclofenac in both VMM39 and SLM2 or in either VMM39 or SLM2 (Fig. 6, group D). Interestingly, there are genes that are strongly downregulated by the drug combination in VMM39 but not in SLM2 (Fig. 6, group A). Finally, there are genes with widely disparate basal expression levels between VMM39 and SLM2 that are similarly dysregulated by the sorafenib and diclofenac combination (Fig. 6, group C). These different patterns of gene expression induced by the drug combination suggest that most transcriptional changes triggered by sorafenib and diclofenac are different in VMM39 and SLM2. We analyzed the annotated gene ontology (GO) terms associated with the transcriptional changes triggered by the sorafenib and diclofenac drug combination to determine if common biologic processes were regulated by the drug combination in VMM39 and SLM2 cells and survival-related GO terms consistently emerge as a common response. Thus, while the different transcriptional response of the 2 cell lines suggests that different mechanisms of drug synergy may be active, there is convergence on common biologic processes.

Discussion

Resistance to targeted therapies can appear after prolonged remission and is often associated with the emergence of mutations that render the target kinase resistant to drug inhibition (6). However, in melanoma and most solid tumors, resistance to therapy often exists *de novo*, sometimes developing in a few weeks or months and often independent of mutations in the target kinase (28–30). It is becoming apparent that redundant, compensatory, and/or survival signaling pathways can rapidly overcome single-point blockade of a signaling pathway (7). This implies that more effective therapies could be achieved by inhibiting a combination of targets like the primary target and a redundant or compensatory target. The classic combinatorial approach for cytotoxic anticancer agents has been to identify agents with different dose-limiting toxicities under the expectation that the combination will allow higher levels of cytotoxic activity in patients. For targeted therapies, however, we have an opportunity to identify biologically effective drug combinations based on the interactions of various signaling pathways (31). Such rational combinations would specifically target complementary signaling components to achieve synergistic outcomes. Some combinations are widely recognized and under development, such as cotargeting the MAPK and PI3K pathways (32, 33). However, this may not be the only or most efficacious combination in every cancer lineage and genetic background. The current understanding of signaling networks limits our ability to rationally explore the range of possibilities. Even for the MAPK pathway, which has been studied in depth for 2 decades, we do not fully understand the ways in which it is connected to other pathways that control cell proliferation and death. Furthermore, our ability to predict the relationships between oncogenic mutations, cell lineage, signaling networks, and therapeutic effectiveness is inadequate.

In this study, we have applied a chemical genetic approach analogous to synthetic lethal screening in yeast genetics to probe the cancer cell-signaling network for novel functional interactions. The prediction is that identifying synergistic lethal effects through effective combinatorial targeting of cooperating oncogenic and survival pathways will achieve robust clinical responses in melanoma and other tumors. Synthetic lethal screens have been applied previously to cancer models and uncovered novel therapeutic targets or compounds (34–36). In these studies, investigators used RNA interference or small-molecule inhibitors to screen cell lines differing in a specific fixed genetic change, such as in an oncogene or tumor suppressor gene. This approach has led successfully to the discovery of unknown synthetic lethal interactions with numerous oncogenes and tumor suppressor genes including *RAS*, *MYC*, *BRCA1*, and *PTEN* (37). This application of synthetic lethality may account for the clinical effectiveness of some small-molecule inhibitors. Cancers may respond to therapies targeting mutations that occur early in cancer development and progression in

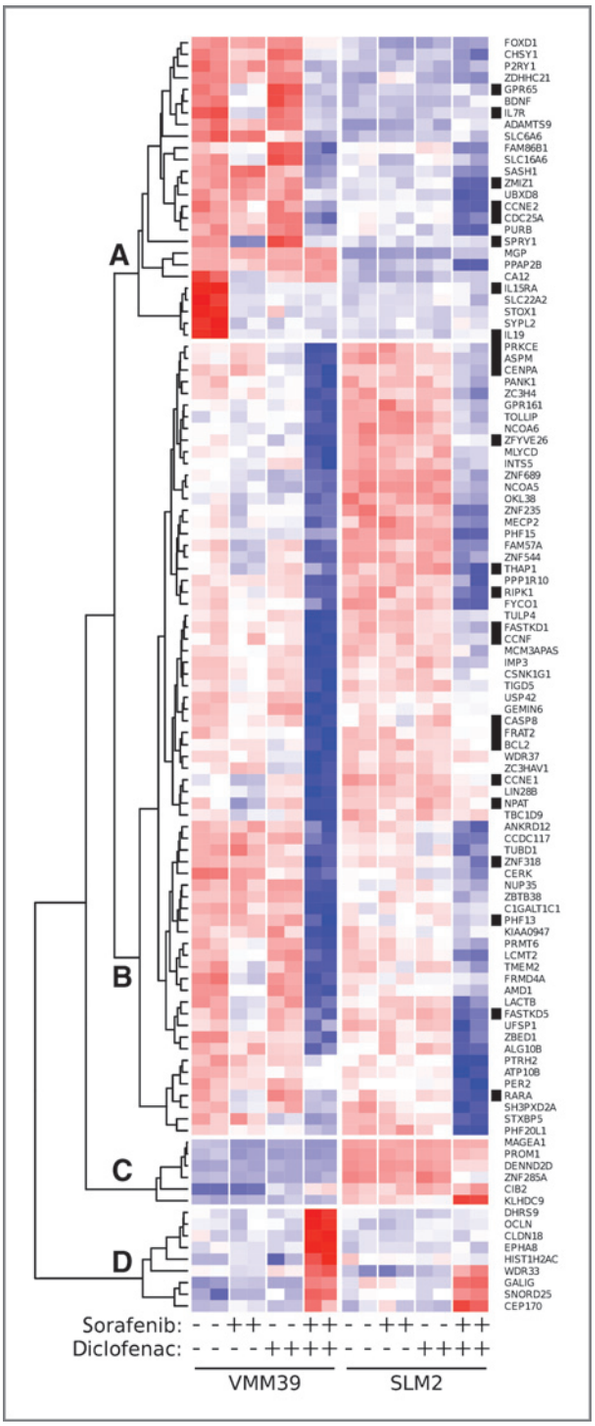

Figure 6. The effect of drug combinations on genome-wide gene expression. Total RNA was isolated from cells (VM339 and SLM2) 24 hours following inhibitor treatment (dimethyl sulfoxide vehicle, sorafenib and diclofenac, both alone and in combination), conducted in duplicate. mRNA abundance was measured by Illumina HT-12 microarray. Genes exhibiting statistically significant (FDR < 0.1%) inhibitor-induced changes were clustered hierarchically by average linkage of scaled cosine correlation similarity, delineating 4 major response patterns: A, genes strongly downregulated by combination inhibition in VMM39, but weakly (or not at all) in SLM2. B, genes downregulated by combination inhibition in both VMM39 and SLM2, with varying magnitude. C, genes with widely disparate basal expression levels between VMM39 and SLM2 that are dysregulated by combination inhibition. D, genes that are upregulated by combination inhibition in either/both VMM39 and SLM2. Black boxes to the left of HUGO gene names denote those genes having annotated associations with survival-related GO terms.

cases where subsequent mutations carry a selective advantage only in the context of the preceding transforming mutations.

Here, we show that a synthetic lethal chemical genetic screen can be used to identify novel synergistic drug combinations. We focused on the combination of sorafenib, a Raf inhibitor with multikinase activity, and the anti-inflammatory COX inhibitor diclofenac. Sorafenib and diclofenac combined synergistically to inhibit the growth of multiple melanoma cell lines. A highly selective MEK inhibitor and a derivative of sorafenib, RAF265, both substituted in part for sorafenib. Similarly, the COX inhibitors celecoxib and ibuprofen both partially substituted for diclofenac. Together, this suggests that the synergistic effect of sorafenib and diclofenac are due, at least in part, to inhibition of RAF and COX. While the drug substitution experiments with different nonsteroidal anti-inflammatory drugs (NSAID) support COX as the relevant molecular target of diclofenac, these experiments are not definitive. We have assessed COX1 and COX2 activity by ELISA but found the basal COX activity in the melanoma lines too low to robustly assess inhibition with NSAIDs (data not shown). Using quantitative PCR (qPCR), we did see COX1 mRNA increase (2×) in VMM39 cells and IL-1β mRNA increase (5×) in DM331 cells with diclofenac consistent with inhibition of COX activity (data not shown; refs. 38, 39). However, we found only a small number of gene expression changes to occur following diclofenac treatment for 8 hours and no changes consistent across both cell lines (Fig. 6). Thus, it is possible that other molecular targets of diclofenac contribute, either in part or whole, to the synergy with sorafenib.

The melanoma cell lines tested were sensitive to the combination of sorafenib and diclofenac independent of the *RAS* and *RAF* mutational status of the melanoma lines. This contrasts with the correlation of sensitivity to single agent RAF and MEK inhibitors in *BRAF* mutant melanomas (40). However, sorafenib is a multikinase inhibitor that targets many kinases in addition to RAF, complicating this interpretation. Further work is required to evaluate fully if drug combinations with agents that target RAF or MEK correlate with *RAS* and *RAF* mutational status in a way similar to the effect of single-agent RAF and MEK inhibitors.

Of the 3 cell lines studied in detail, only DM331, a *RAF* V600E mutant line, showed synergistic inhibition of ERK and cPLA2 signals consistent with interrupting a feed forward signaling loop involving ERK and COX. ERK phosphorylates cPLA2 on serine 505, facilitating cPLA2 activation, which results in the release of arachidonic acid and lysophospholipid from the sn-2 position on

phospholipids (26). COX catalyzes arachidonic acid to prostaglandins that then activate the RAS–RAF–ERK signaling cascade (24, 25, 27). We suggest that, in DM331 melanoma cells, mutationally activated RAF drives ERK activation and subsequent cPLA2 phosphorylation, leading to enhanced arachidonic acid release which feeds forward through prostaglandin production to ERK. The drug combination of sorafenib and diclofenac interrupts this feed forward loop by inhibiting RAF and COX. Consistent with this, the V600E mutant cell lines VMM5A, A375, and SkMel28 also showed synergistic inhibition of ERK activity with the sorafenib and diclofenac combination (data not shown).

The VMM39 cells carrying mutant *RAS* and the SLM2 cells that are wild-type for *RAS* and *RAF* did not show synergistic inhibition of ERK activity in response to the combination of sorafenib and diclofenac, suggesting a different mechanism of synergistic cytotoxicity for this drug combination. It is reasonable that, even when the biologic outcome is the same (i.e., synergistic cytotoxicity), a drug such as sorafenib with multikinase activity would have different mechanisms of action depending on the genetic background of the tumor. Both VMM39 and SLM2 showed little transcriptional change in response to sorafenib or diclofenac alone. Profound statistically significant transcriptional changes were observed when these melanoma cell lines were treated with the combination of sorafenib and diclofenac. These selective transcriptional effects suggest that the cytotoxic effect of the sorafenib and diclofenac drug combination is due to changes in the transcriptional program. A GO term analysis of the transcriptional changes induced by the drug combination indicated that genes involved in cell survival were changing in a drug combination–selective manner. Additional studies are necessary to determine the specific role of these transcriptional changes in the cytotoxic response to sorafenib and diclofenac in the VMM39 and SLM2 melanoma cell lines. Nevertheless, our gene array studies suggest that the underlying signaling networks that control responses to targeted agents can vary substantially depending on the cell genotype. This is likely to complicate attempts to construct combinatorial therapies without a detailed understanding of the mutational status of the cancer cells. Identifying the mechanism of synergy will entail overlaying drug target networks with genomics as well as transcriptomic and proteomic biologic network changes (41, 42). Such a systems approach has been applied with some success (41, 43). As we increase our understanding of cell biologic networks, our ability to rationally select effective drug combinations will continue to improve.

Disclosure of Potential Conflicts of Interest

A. Mackey is employed in HemoShear, LLC as the Director of Bioinformatics. No potential conflicts of interest were disclosed by the other authors.

Authors' Contributions

Conception and design: M.J. Weber, D. Gioeli
Development of methodology: D. Roller, M. Axelrod, M.J. Weber, D. Gioeli
Acquisition of data (provided animals, acquired and managed patients, provided facilities, etc.): D. Roller, D. Gioeli
Analysis and interpretation of data (e.g., statistical analysis, biostatistics, computational analysis): D. Roller, M. Axelrod, B. Capaldo, K. Jensen, A. Mackey, M.J. Weber, D. Gioeli
Writing, review, and/or revision of the manuscript: D. Roller, M. Axelrod, B. Capaldo, K. Jensen, A. Mackey, M.J. Weber, D. Gioeli
Administrative, technical, or material support (i.e., reporting or organizing data, constructing databases): D. Roller, B. Capaldo, A. Mackey, D. Gioeli
Study supervision: M.J. Weber, D. Gioeli
Obtained funding: M.J. Weber, D. Gioeli

Acknowledgments

The authors thank Drs. Kevin Janes and Jason Papin, along with doctoral candidate Paul Jensen, for their insight and helpful discussions on this project.

Grant Support

This work was supported by an award from the Melanoma Research Alliance to M.J. Weber, the Timothy Aycock Melanoma Research Foundation to the UVA Cancer Center, and the NIH Grant R01 CA124706 to D. Gioeli.

The costs of publication of this article were defrayed in part by the payment of page charges. This article must therefore be hereby marked *advertisement* in accordance with 18 U.S.C. Section 1734 solely to indicate this fact.

Received May 4, 2012; revised August 6, 2012; accepted August 26, 2012; published OnlineFirst September 7, 2012.

References

1. Bild AH, Yao G, Chang JT, Wang Q, Potti A, Chasse D, et al. Oncogenic pathway signatures in human cancers as a guide to targeted therapies. Nature 2006;439:353–7.
2. Druker BJ, Talpaz M, Resta DJ, Peng B, Buchdunger E, Ford JM, et al. Efficacy and safety of a specific inhibitor of the BCR-ABL tyrosine kinase in chronic myeloid leukemia. N Engl J Med 2001;344:1031–7.
3. Quigley D, Balmain A. Systems genetics analysis of cancer susceptibility: from mouse models to humans. Nat Rev Genet 2009;10:651–7.
4. Chapman PB, Hauschild A, Robert C, Haanen JB, Ascierto P, Larkin J, et al. Improved survival with vemurafenib in melanoma with BRAF V600E mutation. N Engl J Med 2011;364:2507–16.
5. Roumiantsev S, Shah NP, Gorre ME, Nicoll J, Brasher BB, Sawyers CL, et al. Clinical resistance to the kinase inhibitor STI-571 in chronic myeloid leukemia by mutation of Tyr-253 in the Abl kinase domain P-loop. Proc Natl Acad Sci U S A 2002;99:10700–5.
6. Cortot AB, Janne PA. Resistance to targeted therapies as a result of mutation(s) in the target. In:Gioeli D, editor. Targeted therapies: mechanisms of resistance. New York: Humana Press; 2011. p. 1–31.
7. Gioeli D. The dynamics of the cell signaling network; implications for targeted therapies. In:Gioeli D, editor. Targeted therapies: mechanisms of resistance. New York: Humana Press; 2011. p. 33–53.
8. Kwak EL, Clark JW, Chabner B. Targeted agents: the rules of combination. Clin Cancer Res 2007;13:5232–7.
9. Gioeli D, Wunderlich W, Sebolt-Leopold J, Bekiranov S, Wulfkuhle JD, Petricoin EF III, et al. Compensatory pathways induced by MEK inhibition are effective drug targets for combination therapy against castration-resistant prostate cancer. Mol Cancer Ther 2011;10:1581–90.
10. Bliss C. The toxicity of poisons applied jointly. Ann Appl Biol 1939;26:585–615.

11. Fitzgerald JB, Schoeberl B, Nielsen UB, Sorger PK. Systems biology and combination therapy in the quest for clinical efficacy. Nat Chem Biol 2006;2:458–66.
12. Molhoek KR, Shada AL, Smolkin M, Chowbina S, Papin J, Brautigan DL, et al. Comprehensive analysis of receptor tyrosine kinase activation in human melanomas reveals autocrine signaling through IGF-1R. Melanoma Res 2011;21:274–84.
13. MacConaill LE, Campbell CD, Kehoe SM, Bass AJ, Hatton C, Niu L, et al. Profiling critical cancer gene mutations in clinical tumor samples. PLoS ONE 2009;4:e7887.
14. Smyth GK. Linear models and empirical bayes methods for assessing differential expression in microarray experiments. Stat Appl Genet Mol Biol 2004;3:Article3.
15. Gentleman RC, Carey VJ, Bates DM, Bolstad B, Dettling M, Dudoit S, et al. Bioconductor: open software development for computational biology and bioinformatics. Genome Biol 2004;5:R80.
16. Smyth GK. Limma: linear models for microarray data. In:Gentleman R, Carey V, Dudoit S, Irizarry R, Huber W, editors. Bioinformatics and computational biology solutions using R and bioconductor. New York: Springer; 2005. p. 397–420.
17. Clark JW, Eder JP, Ryan D, Lathia C, Lenz H-J. Safety and pharmacokinetics of the dual action Raf kinase and vascular endothelial growth factor receptor inhibitor, BAY 43-9006, in patients with advanced, refractory solid tumors. Clin Cancer Res 2005;11:5472–80.
18. Auler Júnior JO, Espada EB, Crivelli E, Quintavalle TB, Kurata A, Stolf NA, et al. Diclofenac plasma protein binding: PK-PD modelling in cardiac patients submitted to cardiopulmonary bypass. Braz J Med Biol Res 1997;30:369–74.
19. Kane RC, Farrell AT, Saber H, Tang S, Williams G, Jee JM, et al. Sorafenib for the treatment of advanced renal cell carcinoma. Clin Cancer Res 2006;12:7271–8.
20. Bjorkman DJ. Current status of nonsteroidal anti-inflammatory drugs (NSAID) use in the United States: risk factors and frequency of complications. Am J Med 1999;107:35–85.
21. Bain J, Plater L, Elliott M, Shpiro N, Hastie CJ, McLauchlan H, et al. The selectivity of protein kinase inhibitors: a further update. Biochem J 2007;408:297–315.
22. Karaman MW, Herrgard S, Treiber DK, Gallant P, Atteridge CE, Campbell BT, et al. A quantitative analysis of kinase inhibitor selectivity. Nat Biotechnol 2008;26:127–32.
23. Fabian MA, Biggs WH, Treiber DK, Atteridge CE, Azimioara MD, Benedetti MG, et al. A small molecule-kinase interaction map for clinical kinase inhibitors. Nat Biotechnol 2005;23:329–36.
24. Krysan K, Reckamp KL, Dalwadi H, Sharma S, Rozengurt E, Dohadwala M, et al. Prostaglandin E2 activates mitogen-activated protein kinase/Erk pathway signaling and cell proliferation in non–small cell lung cancer cells in an epidermal growth factor receptor-independent manner. Cancer Res 2005;65:6275–81.
25. Wang D, Buchanan FG, Wang H, Dey SK, DuBois RN. Prostaglandin E2 enhances intestinal adenoma growth via activation of the Ras-mitogen-activated protein kinase cascade. Cancer Res 2005;65:1822–9.
26. Lin LL, Wartmann M, Lin AY, Knopf JL, Seth A, Davis RJ. cPLA2 is phosphorylated and activated by MAP kinase. Cell 1993;72:269–78.
27. Wang D, Dubois RN. Eicosanoids and cancer. Nat Rev Cancer 2010;10:181–93.
28. Villanueva J, Vultur A, Lee JT, Somasundaram R, Fukunaga-Kalabis M, Cipolla AK, et al. Acquired resistance to BRAF inhibitors mediated by a RAF kinase switch in melanoma can be overcome by cotargeting MEK and IGF-1R/PI3K. Cancer Cell 2010;18:683–95.
29. Johannessen CM, Boehm JS, Kim SY, Thomas SR, Wardwell L, Johnson LA, et al. COT drives resistance to RAF inhibition through MAP kinase pathway reactivation. Nature 2010;468:968–72.
30. Nazarian R, Shi H, Wang Q, Kong X, Koya RC, Lee H, et al. Melanomas acquire resistance to B-RAF(V600E) inhibition by RTK or N-RAS upregulation. Nature 2010;468:973–7.
31. Dancey JE, Chen HX. Strategies for optimizing combinations of molecularly targeted anticancer agents. Nat Rev Drug Discov 2006;5:649–59.
32. Kinkade CW, Castillo-Martin M, Puzio-Kuter A, Yan J, Foster TH, Gao H, et al. Targeting AKT/mTOR and ERK MAPK signaling inhibits hormone-refractory prostate cancer in a preclinical mouse model. J Clin Invest 2008;118:3051–64.
33. Engelman JA, Chen L, Tan X, Crosby K, Guimaraes AR, Upadhyay R, et al. Effective use of PI3K and MEK inhibitors to treat mutant Kras G12D and PIK3CA H1047R murine lung cancers. Nat Med 2008;14:1351–6.
34. Barbie DA, Tamayo P, Boehm JS, Kim SY, Moody SE, Dunn IF, et al. Systematic RNA interference reveals that oncogenic KRAS-driven cancers require TBK1. Nature 2009;462:108–12.
35. Scholl C, Fröhling S, Dunn IF, Schinzel AC, Barbie DA, Kim SY, et al. Synthetic lethal interaction between oncogenic KRAS dependency and STK33 suppression in human cancer cells. Cell 2009;137:821–34.
36. Luo J, Emanuele MJ, Li D, Creighton CJ, Schlabach MR, Westbrook TF, et al. A genome-wide RNAi screen identifies multiple synthetic lethal interactions with the Ras oncogene. Cell 2009;137:835–48.
37. Chan DA, Giaccia AJ. Harnessing synthetic lethal interactions in anticancer drug discovery. Nat Rev Drug Discov 2011;10:351–64.
38. Yano A, Higuchi S, Tsuneyama K, Fukami T, Nakajima M, Yokoi T. Involvement of immune-related factors in diclofenac-induced acute liver injury in mice. Toxicology 2012;293:107–14.
39. Lu X, Xie W, Reed D, Bradshaw WS, Simmons DL. Nonsteroidal antiinflammatory drugs cause apoptosis and induce cyclooxygenases in chicken embryo fibroblasts. Proc Natl Acad Sci U S A 1995;92:7961–5.
40. Solit DB, Garraway LA, Pratilas CA, Sawai A, Getz G, Basso A, et al. BRAF mutation predicts sensitivity to MEK inhibition. Nature 2006;439:358–62.
41. Chua HN, Roth FP. Discovering the targets of drugs via computational systems biology. J Biol Chem 2011;286:23653–8.
42. Azmi AS, Wang Z, Philip PA, Mohammad RM, Sarkar FH. Proof of concept: network and systems biology approaches aid in the discovery of potent anticancer drug combinations. Mol Cancer Ther 2010;9:3137–44.
43. Cokol M, Chua HN, Tasan M, Mutlu B, Weinstein ZB, Suzuki Y, et al. Systematic exploration of synergistic drug pairs. Mol Syst Biol 2011;7:544.